Atmospheric Environment 126 (2016) 21–27

Contents lists available at ScienceDirect

Atmospheric Environment

journal homepage: www.elsevier.com/locate/atmosenv

The contribution of dust devils and dusty plumes to the aerosol budget in western China

Yongxiang Han [a, b], Kanghong Wang [a], Feng Liu [c, *], Tianliang Zhao [a], Yan Yin [a], Jiapeng Duan [a], Zhaopeng Luan [a]

[a] Collaborative Innovation Center on Forecast and Evaluation of Meteorological Disasters/Key Laboratory of Meteorological Disaster, Ministry of Education, Nanjing University of Information Science and Technology, Nanjing 210044, China
[b] Key Laboratory for Aerosol-Cloud-Precipitation of China Meteorological Administration, Nanjing University of Information Science and Technology, Nanjing 210044, China
[c] Climate and Atmospheric Science Section, Division of Illinois State Water Survey, Prairie Research Institute, University of Illinois at Urban-Champaign, Champaign, IL 61820, USA

HIGHLIGHTS

- Dust aerosols come from dust storms and DDDP (dust devils and dust plumes).
- Diurnal variability and Seasonal.
- Thermodynamic efficiency can represent this variation.
- 53% of total annual desert dust in western China comes from DDDP.
- DDDP affect climate more than dust storms.

ARTICLE INFO

Article history:
Received 5 March 2015
Received in revised form
9 November 2015
Accepted 12 November 2015
Available online 29 November 2015

Keywords:
Dust devil
Dusty plumes
Dust aerosol
Variation characteristics
Thermodynamic efficiency
Contribution rate

ABSTRACT

Based on thermodynamic theory and comprehensive analyses of the Total Ozone Mapping Spectrometer Aerosol Index, surface micro-pulse LiDAR, meteorological elements in the atmospheric boundary layer, observations of sporadic dust devil, the diurnal and seasonal changes of dust devil are characterized, the contribution to the aerosol budget from dust devils and dusty plumes is quantitatively analyzed. The results show that: 1) dust devils and dusty plumes show obvious diurnal and seasonal variations with a single-peaked distribution; 2) thermodynamic efficiency can effectively account for the daily variations of dust devils and dusty plumes from morning to early afternoon, seasonal changes of dust devil activity in summer. The future improved thermodynamic efficiency could be applied to their parameterization; 3) dust devils and dusty plumes may contribute more than 53% of annual total dust aerosols over desert regions in western China,but the calculated contributions have uncertainties. It will be helpful to understand the dust devil and dusty plume contributions to global and regional aerosol loading.
Published by Elsevier Ltd.

1. Introduction

Dust aerosols are the main aerosol constituent of the atmosphere, accounting for nearly half the total aerosols in the troposphere (Shi and Zhao, 2003; Han et al., 2008). Dust aerosols play an important role in climate change (Duce et al., 1980; Martin, 1990; Bishop et al., 2002; Han et al., 2011), and dust storms is often thought to be responsible for the amount of dust aerosols (Duce et al., 1980; Aoverpeck et al., 1996; Han et al., 2009). The emission mechanism of dust storm is associated with dynamics under large-scale gale conditions, such as atmospheric depressions and mobile cyclones (Fiedler et al., 2014); nocturnal low level jets (Heinold et al., 2015); and cold pool outflows from convective storms (Roberts and Knippertz, 2014).

However, although dust storms can uplift vast quantities of dust aerosols into the atmosphere, dust storms are still low-probability events (Han et al., 2008). Therefore, the total amount of dust aerosols in the atmosphere provided by dust storms may present

* Corresponding author. Environmental Programs, Maricopa Association of Governments, 302 North 1st Avenue Suite 300, Phoenix, AZ 85003, USA.
E-mail address: fengliu.us@gmail.com (F. Liu).

http://dx.doi.org/10.1016/j.atmosenv.2015.11.025
1352-2310/Published by Elsevier Ltd.

an incomplete picture.

The small-scale processes such as dust devils and dusty plumes (DDDP) also can lift the dust aerosols into the atmosphere (Koch and Renno, 2005). On sunny days with weak winds, solar radiation increases the ground sensible heat flux, causing the ground air temperature to rise and the air density to drop. Under certain conditions of angular momentum, will form and carry dust aerosols into the atmosphere (Gu et al., 2010). The emission mechanism of DDDP is normally related to thermodynamic under sunny conditions with weak winds (Renno et al., 1998; Leovy, 2003). The typical dust devils are generally 10 m in diameter with a typical duration of several minutes, while large dusty non-rotating convective plumes are generally 100 m in diameter and persist for nearly an hour (Koch and Renno, 2005). Dust devils are common small-scale dust transport systems in the Gobi Desert region and over dry plowed fields (Koch and Renno, 2005). The DDDP caused by thermal turbulence essentially may be used for quantifying the dust aerosols in non-dust storm seasons over deserts and adjacent areas. The authors Han et al. (2008) and Deng et al. (2009) demonstrated that high concentrations of dust aerosols can be observed in the troposphere on sunny days during non-dust storm periods. Approximately 250 dust devils can be observed per km^2 in the Mojave Desert of southern California (Ryan and Carroll, 1970), and a large dust devil can uplift approximately 1800 kg of dust into the atmosphere in southern Navada according to estimates by Metzger (1999). The DDDP possess a tremendous potential for uplifting dust from the surface into the atmosphere (Gu et al., 2010). Researchers have calculated that DDDP may contribute to approximately 35% of global dust aerosols (Koch and Renno, 2005), as much as 65% in the United States (Gillette and Sinclair, 1990; Koch and Renno, 2005) showed that DDDP play an important role in the earth's aerosol budget. Han et al. (2008) even argued that dust devils dominate the aerosol budget in the deserts of western China. It suggested that although the dust emissions caused by a single dust devil and convective plume are much smaller than that by a dust storm, the total amount of dust lifted annually by DDDP should be significant. However, Jemmett-Smith et al. (2015) provided much lower global emissions caused by dust devils and dusty plumes compared to others. The substantial uncertainties of emission estimations by DDDP imply that mechanisms of dust flux caused by dust devil are important but poorly understood.

Observations of DDDP are very rare due to their sporadic appearance and mobility, and previous studies on dust devils are normally based on single dust devil events and numerical simulations. The numerical simulations have provided some key findings (Cortese and Balachandar, 1993; Shapiro and Kogan, 1994; Kanak et al., 2000; Toigo, 2003; Kanak, 2005; Gu et al., 2008, 2010) and given insight into vortex dynamics within the boundary layer (Leovy, 2003). However, the variation in climatological characteristics of DDDP has not yet been fully understood. In this paper, based on comprehensive analyses of the Total Ozone Mapping Spectrometer Aerosol Index (TOMS-AI), surface micro-pulse LiDAR, meteorological elements, and the atmospheric boundary layer in association with sporadic dust devil observed from western China, the diurnal and seasonal characteristics of dust devils are well analyzed. Furthermore, the annual total distributions of dust aerosols produced by DDDP are also estimated. This research provides the potential to advance the understanding of climate effects of aerosol loading due to dust devil activities.

2. Study area and methodology

The study area is located in northwestern China. The region covers Taklimakan, Gurbantunggut, Kumtag, Badain Jaran, Tengger, Ulan Buh, Hobq, Mu Us, Onqin Daga, and Horqin, forming an east-west mid-latitude desert belt (Fig. 1). The desert area covers 1.5×10^6 km^2, approximately 15.9% of the land area of China (Sun et al., 1998).

The daily TOMS-AI data from 1979 to 2005 (http://toms.gsfc.nasa.gov/aerosols/aerosols.html) were used to estimate an index of total dust amount over desert areas with a spatial resolution of 1.25° longitude and 1° latitude, which has been widely used in dust research (Alpert et al., 2006). Although the data were not available between May 1993 and September 1996 due to the replacement of two satellites, cloudy regions are very limited over the whole research area which is covered by roughly 133 TOMS AI pixels. Surface temperature, depth of the convection boundary layer, and solar radiation were cited from the literature (Qiao et al., 2010; Li et al., 1999; 2011; Zhang et al., 2004; 2011; Hui et al., 2011). Observed data for dust devils from 1964 to 1970 in the Peafowl River basin, located on the northeastern margin of the Taklimakan, were compiled from the reference (Lue, 1983). In addition, during April 2008, the diurnal vertical distribution of dust aerosols was obtained from observations by surface micro-pulse LiDAR at Minqin in the southern Tengger Desert, China.

A simple thermodynamic theory for dust devils proposed by Renno et al. (1998) states that the dust devil strength depends on the thermodynamic efficiency, η (Koch and Renno, 2005):

$$\eta = \frac{\Gamma_{ad} Z_{CBL}}{T_h}, \tag{1}$$

where Z_{CBL} is the height of the convection boundary layer,T_h is the surface temperature, and Γ_{ad} is the adiabatic lapse rate ($\Gamma_{ad} = 10\ K\ km^{-1}$).

The fractional area covered by DDDP is estimated by σ:

$$\sigma \approx \left(\frac{\mu}{\eta}\right)^{1/2} \left(\frac{\Delta p}{\rho_{air} g T_R}\right)^{3/2} \left(\frac{F_{in}}{\rho_{air}}\right)^{-1/2}, \tag{2}$$

where μ is a dimensionless coefficient of turbulent dissipation of mechanical energy,$\mu \approx 12-24$ and the pressure difference from the surface to the convection boundary layer is $\Delta p = \rho_{air} g Z_{CBL}$, where the air density ρ_{air} is 1 kgm^{-3}, the acceleration of gravity g is 9.8 gm^{-2}, F_{in} is the heat input to the convective heat engine,$F_{in} \approx 11 \pm 5\ kW\ m^{-2}$, and the radiative timescale of the convective boundary layer T_R is 9×10^5 s (Koch and Renno, 2005).

The total dust emissions (DAE_{tot}) by DDDP can be estimated by:

$$DAE_{tot} = D_{time} \times S \times \sigma \times F_d \tag{3}$$

Where F_d is the estimated dust fluxes, D_{time} is the duration of DDDP, S is the area which expected to serve as a source of loose particles that can easily be uplifted into the atmosphere (Sinclair, 1969; Balme and Greeley, 2006; Oke et al., 2007).

3. Results

3.1. Diurnal variability of dust devils

According to the thermodynamic theory, atmospheric convection strength depends on thermodynamic efficiency (η) (Renno and Ingersoll, 1996; Renno et al., 1998; 2004; Renno, 2008). The observational datasets used for calculating η include convection boundary layer height and surface temperature from field experiments in Dunhuang in summer (Zhang et al., 2004; Li et al., 2011). The results (Fig. 2) show that η characterized by an obviously diurnal cycle with a single-peaked distribution. Before 09:00 LST (Local Standard Time), η was less than1%. After 09:00 LST, η began to increase rapidly up to a maximum at 14:00 LST, then it began to

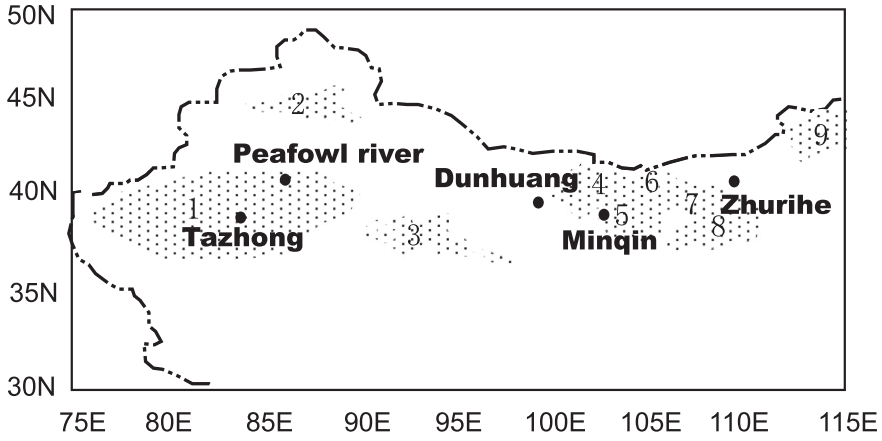

Fig. 1. Distribution of deserts and location of observation stations in northern China. Note: 1,Taklimakan; 2,Gurbantunggut; 3,Kumtag; 4,Badain Jaran; 5,Tengger; 6,Ulan Buh; 7,Hobq; 8,Mu Us; 9,Onqin Daga.

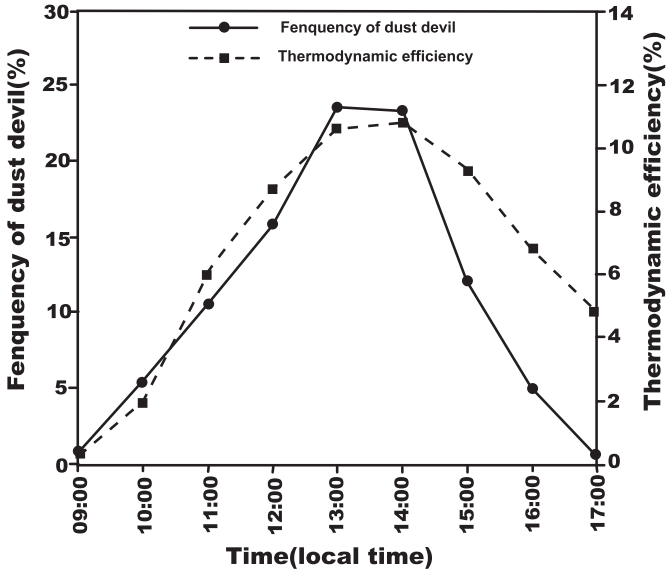

Fig. 2. Diurnal changes in the thermodynamic efficiency of dust devils and the frequency of dust devils at Peafowl River.

decrease. However, the diurnal cycle of dust devils according to η has not been validated by field observations so far.

According to 193 dust devil occurrences visually observed near the Peafowl River from 1964 to 1970 (Lue, 1983), the frequency of dust devils with diameter greater than 2 m had almost the same diurnal variation as η, as clearly shown in Fig. 2. The Pearson correlation coefficient of 0.86 indicates the high association between the two variables ($p < 0.01$, passing the 0.01 statistical test criterion). The both reached maximum values at about 14:00 LST. Meanwhile, there is a notable discrepancy from 14:00 onwards, which appears to extend beyond 17:00, the η decreases more slowly than the frequency of dust devils after 14:00 LST. It implied that the η may be not able to reflect complicate situation of CBL in later afternoon compared with observed occurrences of dust devils. Dust devils occurred frequently from 11:00 to 16:00 LST, during which approximately 65% of the daily total number of dust devils were observed. No dust devils appeared before 9:00 LST and after 18:00 LST during field observations.

Because of the sporadic appearance and mobility of dust devils, direct observations of dust devil are lacking. One indirect method may be discovery of dust devil traces. Assume that the total amount of dust aerosols comes from dust storms, and DDDP, if the contribution by dust storms is eliminated from total dust aerosols, the remainder should be resulted from DDDP. During April 2008, there were no dust storms observed at Minqin station or in its adjacent area according to the Real-time dust storms data per 3 h from http://data.cma.gov.cn/data by MICAPS (Meteorological Information Comprehensive Analysis And Process System), and thus the average diurnal vertical distribution of dust aerosols over this region, quantified through extinction coefficient derived from measurements from surface micro-pulse LiDAR, can be account for the contribution of DDDP. The averaged diurnal variability of the extinction coefficient over the Minqin station was calculated from the LiDAR data in April. The results as illustrated in Fig. 3 showed the similar characteristics of diurnal variation of the extinction coefficient with a peak value between 12:00 and 14:00 LST. The major difference between Figs. 2 and 3 is that the Fig. 3 represented the background dust aerosols before 9:00 LST and after 18:00 LST. This implies that the residual dust aerosols caused by daily dust devils be the background dust aerosols during night due to stable boundary layer conditions, but that still needs to be confirmed by observations and further study. However, the results demonstrate that thermodynamic efficiency (η) is able to represent the daily, actually from morning to early afternoon, variation of dust devils.

3.2. Seasonal variability of dust devils

The distribution of calculated η by running monthly average presents a single peak (Fig. 4). The value of η increased from winter to summer and reached a maximum in July, and then decreased from autumn to winter with a minimum in December. The similar monthly variation characteristics of η can be found when we compared to dust devil occurrences near the Peafowl River (Lue, 1983). The Pearson correlation coefficient of 0.86 indicates the high association between the two variables ($p < 0.01$, passing the 0.01 statistical test criterion). Note that the frequency of dust devils in April was less than in March and the peak occurred in June rather than in July as the monthly η. The reason for this discrepancy is because April is the dust storms season (Song et al., 2004). The frequency of winds in excess of 17 m/s is the largest in April (Wang, 2011), and it is not suitable for formation of DDDP which mostly occurs in the favorable conditions of sunny and weak winds. The discrepancy indicates the weakness of η theory that it is not able to

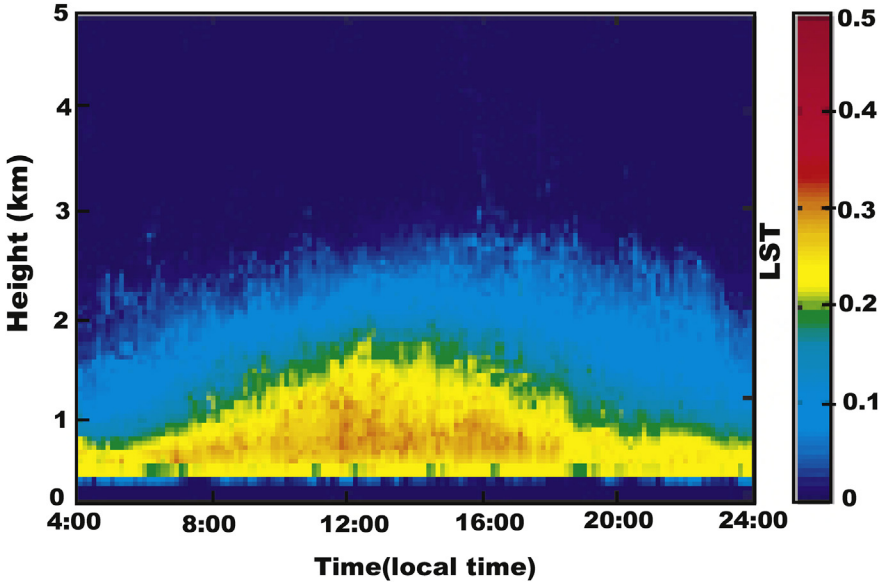

Fig. 3. Average extinction coefficient of the aerosol distribution over the Minqin station during April 2008.

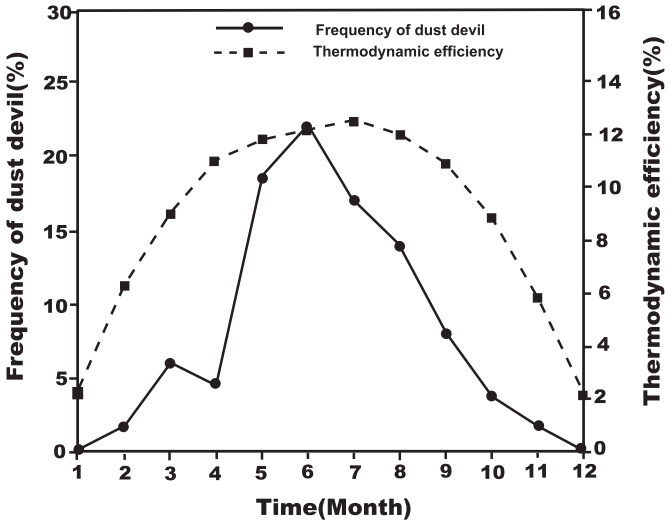

Fig. 4. Monthly changes in the frequency and thermodynamic efficiency of dust devils.

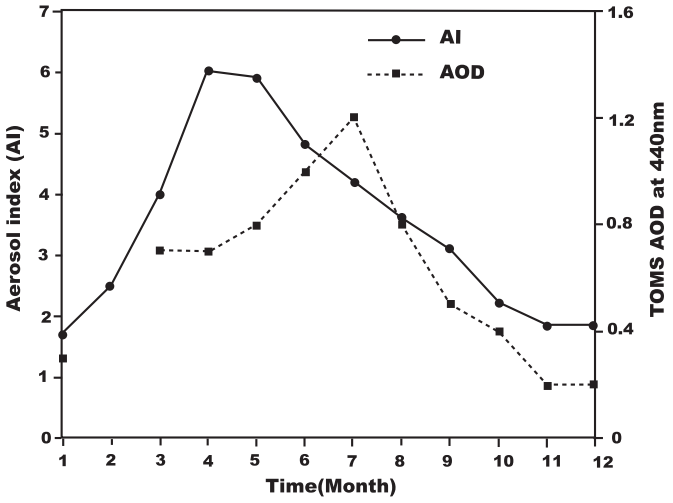

Fig. 5. Monthly averages of TOMS-AI over desert areas in northern China and 440-nm optical thickness at Tazhong station.

identify the high wind period dominated by dust storms. The η may need to be updated later by wind restraint factor.

TOMS-AI can accurately reflect dust aerosols in desert regions (Alpert et al., 2006). In the absence of dust storms, the TOMS-AI data gives the contribution by DDDP. Fig. 5 shows almost the similar monthly variation characteristics as Fig. 4, but the peak values appear during April and May when dust storms were dominant. However, when the effects of dust storms were eliminated from a 440-nm optical thickness at an observation station in the center of the Taklimakan Desert named Tazhong (Li et al., 1999), the monthly variation in optical thickness remained remarkably consistent with that of monthly η.

Although the time of peak occurrence showed slight shifted, these four different approaches outlined the monthly variability characteristics of DDDP. Despite some errors, these results approve that the thermodynamic efficiency (η) can roughly represent the monthly variation of dust devils. It does work very well in summer.

3.3. Estimated dust emissions of DDDP in the Taklimakan Desert

The dust emissions of DDDP were calculated according to Equation (1). For a standard dust devil and a dust plume, the average vertical dust flux values (F_d) were 0.7 gm^{-2} s^{-1} and 0.1 gm^{-2} s^{-1}, respectively, and the maximum and minimum values were 1.13 gm^{-2} s^{-1} and 0.47 gm^{-2} s^{-1} (Koch and Renno, 2005). The σ can be calculated according to Equation (2). The area of the total sources of loose dust particles that can easily be uplifted into the atmosphere is 33.76×10^{10} m^2 × 85% in the Taklimakan Desert (Gao et al., 2008). The duration of DDDP was calculated according to the average day length (Table 1) because the DDDP occur in the day time.

The calculated monthly dust emissions by DDDP (Table 1) showed an obviously monthly variation with a single-peak distribution and the peak occurring in July. From January to July, the average dust emissions increased continuously and reached a

Table 1
Estimated monthly dust aerosol emissions by DDDP.

Month	S × σ km^2	Day length 10^4 s	Average 10^6 t	Maximum 10^6 t	Minimum 10^6 t
1	2.38	3.42	1.955	2.754	1.139
2	5.865	3.84	5.44	7.65	3.145
3	6.29	4.32	6.545	9.18	3.825
4	8.245	4.7	9.35	12.75	5.27
5	9.095	5.22	11.39	13.09	5.44
6	9.605	5.4	12.41	17.51	7.225
7	9.945	5.4	12.835	18.19	7.565
8	9.35	5.04	11.305	15.98	6.63
9	8.585	4.5	9.35	13.09	5.44
10	6.545	3.96	6.205	8.755	3.655
11	4.165	3.6	3.57	5.1	2.125
12	2.04	3.24	1.615	2.235	0.935

maximum value in July. For seasonal variations, the dust emissions was 2.73 × 10^7 t in spring, 3.66 × 10^7 t in summer, 1.91 × 10^7 t in autumn, and 9.01 × 10^6 t in winter. The annual average, maximum, and minimum dust emissions were 9.18 × 10^7 t, 2.38 × 10^8 t, and 9.86 × 10^7 t, respectively.

3.4. Estimated annual dust emissions from dust storms and DDDP in the Taklimakan Desert

In the Taklimakan Desert, dust storms frequently occur in the Desert and can uplift vast quantities of dust aerosols into the atmosphere (Han et al., 2008). To estimate the potential dust emissions generated by dust storms, the average vertical emission dust flux and the duration of each dust storm were investigated. Dust storms occurred 88 times from 1997 to 2002 with a total duration of 306.61 h, thus the annual average duration was 51.1 h in the Taklimakan Desert (Li et al., 2006). The actual value of vertical dust emission flux cannot be observed directly, but it can be estimated according to previous researchers. The Table 2 shows the results of calculated average vertical dust emission flux. It can be seen that the flux ranges from 40.07 × 10^{-7} kg/(m^2·s) to 9.95 × 10^{-9} kg/(m^2·s) and covers 2–3 orders of magnitude.

Assuming that dust storms sweep across the whole Taklimakan Desert with the area of 33.76 × 10^{10} m^2 in the fraction of 85% mobile sand dunes (Gao et al., 2008), and the annually duration of all dust storms is 51.1 h or 51.1 × 3600 s as aforementioned, the potential total dust emissions by dust storms could be calculated according to the various vertical emission flux values (also shown in Table 2). The highest and lowest annually potential total dust emissions from dust storms are 2.125 × 10^8 t and 5.1 × 10^5 t, respectively. The averaged potential emission is 4.41 × 10^7 t.

Previous studies (Han et al., 2008; Deng et al., 2009) have indicated that the total amount of atmospheric dust aerosols depends mainly on dust storms and DDDP. The total amounts of atmospheric dust aerosols in the Taklimakan Desert were then calculated as: 1) maximum 4.505 × 10^8 t (DDDP 2.38 × 10^8 t, dust storms 2.125 × 10^8 t); 2) minimum 9.91 × 10^7 t (DDDP 9.86 × 10^7 t, dust storms 5.1 × 10^5 t); average 1.359 × 10^8 t (DDDP 9.18 × 10^7 t, dust storms 4.41 × 10^7 t). Therefore, contribution of DDDP to the annually total dust emissions is at least approximately 52.8% in the Taklimakan Desert. In addition, according to the cumulative total values of TOMS-AI for dust storms and non-dust storms over 22 years, dust devils were shown to contribute approximately 58% of total dust aerosols over desert regions in northern China (Deng et al., 2009). Two results based on different approaches have therefore shown that dust devils can contribute more than half of the total dust aerosols over desert regions in western China. This suggests that the DDDP contributions to global and regional aerosol loadings should not be ignored and could be significant and comparable to that from dust storms.

Table 2
Vertical emission dust flux and total dust by dust storm in various regions of the Gobi Desert in China.

Flux (kg/(m^2·s))	Location	Time	Reference	Total dust (t)
40.07 × 10^{-7}	Tazhong	2008-07-19	Yang et al., 2010	2.125 × 10^8
7.52 × 10^{-8}	Zhurihe	2006-03-26	Shen et al., 2008	3.995 × 10^6
4.27 × 10^{-8}	Zhurihe	2006-04-06	Shen et al., 2008	2.295 × 10^6
1.58 × 10^{-8}	Dunhuang	2002-04-13	Shen et al., 2003	1.36 × 10^6
9.95 × 10^{-9}	Dunhuang	2002-04-08	Shen et al., 2003	5.1 × 10^5

However, the calculated contributions from DDDP and from dust storm have uncertainties because of the scarce observations and assumed parameters. As sources of uncertainties of emission estimations, the following assumptions are applied in this paper: 1) the total dust aerosol is the summation of dust aerosols caused by dust storms, dust devils and dusty plumes in the desert regions (Koch and Renno, 2005). Other dust emission sources are not known, and their contributions could not be taken into account. 2) There are several options for vertical dust flux (Koch and Renno, 2005; Metzger et al., 2011; Neakrase and Greeley, 2010), choose different values will be leading to different results which also shows a certain uncertainty. We try to estimate an upper bound to the uncertainties in this study by citing the higher values from Koch and Renno (2005). The higher values will greatly increase estimation of dust emissions by DDDP. For example, Jemmett-Smith et al. (2015) recently estimates global emissions caused by dust devils and dusty plumes, and the result is much lower compared to that based on Koch and Renno (2005). 3) Another source of uncertainty is the calculation of the area of dust sources. In this paper, the area of mobile sand dunes with 85% of Taklimakan Desert was adopted. It accounts for more than 85% of the whole desert area because the fine sand with particle size from 0.065 to 0.25 nm extremely accounted for more than 85% of the total sand (Gao et al., 2008). These fine particles are easily picked off the desert surface and uplifted into the atmosphere by wind. In addition, although the typical dust storms cover only a small fraction of the desert, but in order to estimate the upper limit of sandstorm emissions, the same area of mobile sand dunes is applied in this study, Finally, the long-term seasonal changes of dust sources (Ginoux et al., 2012) are not considered in this paper.

4. Conclusions

The contribution to the total dust aerosols from dust devils and dust plumes has been estimated based on multiple observational datasets. The results can be summarized as follows:

1). Dust devils show obvious diurnal and monthly variations with single-peak distributions. The daily occurrence frequency and dust emission peaks around 12:00–14:00 (LST), while the monthly one reaches the highest value in summer.
2). The observed dust aerosol loading during night, considered as a kind of background dust aerosol, reflects the lag effects of day-time dust aerosols. The residual day-time dust aerosols are trapped in the shallow and stable nocturnal boundary layer because turbulent mixing processes tends to be suppressed after sunset.
3). Thermodynamic efficiency (η) can roughly represent the diurnal and monthly variation of dust devils. But due to the assumed constant lapse rate the η could not reflect complicated situation of convective boundary layer in the later afternoon. For the purpose of application of thermodynamic efficiency to the parameterization of dust emissions caused by dust devils and dusty plumes, the improvement of thermodynamic efficiency will be one of central focuses in our future work.
4). On an annual basis, dust devils and dusty plumes can contribute more than 53% of total dust aerosols over desert regions in China. This implies that dust devils and dusty plumes may play a comparable or even more important role than dust storms not only in West China but also possible in global and regional scale. However, the calculated contributions from DDDP and from dust storm have uncertainties

Acknowledgments

This study has been co-supported by the National Natural Science Foundation of China (41375158; 41030962). We would also like to thank all reviewers for their helpful comments and suggestions, which have led to improvements of this paper. Any opinions, findings, and conclusion or recommendations expressed in this material are those of the authors and do not necessarily reflect the view of the Nanjing University of Information Science and Technology, University of Illinois at Urban-Champaign, or any organizations and governmental agencies.

References

Alpert, P., Barkan, J., Kishcha, P., 2006. A potential climatic index for total Saharan dust: the Sun in solation. J. Geophys. Res. 111. D01103.1–D01103.8.
Aoverpeck, J.T., Rind, D., Lacis, A., et al., 1996. Possible role of dust-induced regional warming in abrupt climate change during the last glacial period. Nature 384, 447–449.
Balme, M., Greeley, R., 2006. Dust devils on Earth and Mars. Rev. Geophys. 44 (3). RG3003, 1–22.
Bishop, J.K.B., Davis, R.E., Sherman, J.T., 2002. Robotic observations of dust storm enhancement of carbon biomass in the North Pacific. Science 298, 817–821.
Cortese, T., Balachandar, S., 1993. Vertical nature of thermal plumes in turbulent convection. Phys. Fluids A5, 3226–3232.
Deng, Zuqin, Han, Yongxiang, Bai, Huzhi, Zhao, Tianliang, 2009. Reason analysis of the dust aerosols' content change in desert regions. China Environ. Sci. 29 (12), 1233–1238.
Duce, R.A., Unni, C.K., Ray, B.J., Prospero, J.M., Merrill, T., 1980. Long-range atmospheric transport of soil dust from Asia to the tropical North Pacific: temporal variability. Science 209, 1522–1524.
Fiedler, S., et al., 2014. How important are atmospheric depressions and mobile cyclones for emitting mineral dust aerosol in North Africa? Atmos. Chem. Phys. 14 (17), 8983–9000.
Ginoux, P., Prospero, J.M., Gill, T.E., Hsu, N.C., Zhao, M., 2012. Global-scale attribution of anthropogenic and natural dust sources and their emission rates based on MODIS deep blue aerosol products. Rev. Geophys. 50 http://dx.doi.org/10.1029/2012RG000388. RG3005.
Gao, Weidong, Yuan, Yujiang, Liu, Zhihui, Wei, Wenshou, 2008. Status of dust sources and aerosol formatting condition analysis in Xinj iang. J. Desert Res. 28 (5), 968–973.
Gillette, D., Sinclair, P.C., 1990. Estimation of suspension of alkaline material by dust devils in the United States. Atmos. Environ. 24, 1135–1142.
Gu, Zhaolin, et al., 2008. Analysis on dust devil containing loess dusts of different sizes. Aerosol Air Qual. Res. 8 (01), 65–77.
Gu, Zhaolin, Wei, Wei, Zhao, Yongzhi, 2010. An overview of surface conditions in numerical simulations of dust devils and the consequent near-surface air flow fields. Aerosol Air Qual. Res. 10, 272–281.
Han, Yongxiang, Fang, Xiaomin, Zhao, Tianliang, Bai, Huzhi, Kang, Shichang, Song, Lianchun, 2009. Suppression of precipitation by dust particles originated in the Tibetan Plateau. Atmos. Environ. 43, 569–574.
Han, Y., Dai, X., Fang, X., Chen, Y., Kang, F., 2008. Dust aerosol. A possible accelerant for the arid climate in North China. J. Arid Environ. 1476–1489.
Han, Yongxiang, Tianliang, Zhao, Song, Lianchun, Fang, Xiaomin, Yin, Yan, Deng, Zuqin, Wang, Suping, Fan, Shuxian, 2011. A linkage between Asian dust,dissolved iron and marine export production in the deep ocean. Atmos. Environ. 45, 4291–4298.
Heinold, Bernd, Knippertz, Peter, Beare, Robert J., 2015. Idealized largeeddy simulations of nocturnal low level jets over subtropical desert regions and implications for dustgenerating winds. Q. J. R. Meteorol. Soc. 141, 1740–1752.
Hui, Xiaoying, Gao, Xiaoqing, Wei, Zhigang, et al., 2011. Analysis on the determination of boundary layer height in daytime Dunhuang summer using ascent rate of sounding balloon. Plateau Meteorol. 30 (03), 614–619.
Jemmett-Smith, B.C., Marsham, J.H., Knippertz, P., Gilkeson, C.A., 2015. Quantifying global dust devil occurrence from meteorological analyses. Geophys. Res. Lett. 42, 1275–1282. http://dx.doi.org/10.1002/2015GL063078.
Kanak, K.M., Lil1y, D.K., Snow, J.T., 2000. The formation of vertical vortices in the convective boundary layer. J. Q. J. Roy. Meteor Soc. 126, 2789–2810.
Kanak, K.M., 2005. Numerical simulation of dust devil-scale vortices. J. Q. J. Roy. Meteor. Soc. 131, 1271–1292.
Koch, J., Renno, N.O., 2005. The role of convective plumes and vortices on the global aerosol budget. Geophys. Res. Lett. 32 (18). L18806 (1-5).
Leovy, C.B., 2003. The devil is in the dust. Nature 424, 1008–1009.
Li, Hu, Li, Xia, Xiao, Jidong, et al., 1999. The monitoring for sand-storm in center of Taklamagan Desert by using remote sensing. J. Xinjiang Agric. Univ. 22 (3), 219–223.
Li, Shengyu, Lei, Jiaqiang, Xu, Xinwen, et al., 2006. Features of sandstorms in hinterland of Taklmiakan Desert: a case of Tazhong area. J. Nat. Disasters 2, 14–19.
Li, Yanying, Zhang, Qiang, Xue, Xinling, et al., 2011. Relationship between atmosphere boundary layer characteristics and sand-dust weather climatology in Minqin. J. Desert Res. 3, 757–764.
Lue, 1983. The dust devils on the south Gobi of Xinjiang. Meteorol. Mon. 4, 33.
Martin, J.H., 1990. Glacial-interglacial CO2 change: the iron hypothesis. Paleoceanography 5, 1–13.
Metzger, S.M., 1999. Dust Devils Are Aeolian Transport Mechanisms in Southern Navada and in the Mars Pathfinder Landing Site. Ph.D. Dissertation. University of Nevada, Reno, Reno.
Metzger, S.M., Balme, M.R., Towner, M.C., Bos, B.J., Ringrose, T.J., Patel, M.R., 2011. In situ measurements of particle load and transport in dust devils. Icarus 214, 766–772. http://dx.doi.org/10.1016/j.icarus.2011.03.013.
Neakrase, L.D., Greeley, R., 2010. Dust devil sediment flux on Earth and Mars: laboratory simulations. Icarus 206 (1), 306–318.
Oke, A.M.C., Tapper, N.J., Dunkerley, D., 2007. Willy willies in the Australian landscape: the role of key meteorological variables and surface conditions in defining frequency and spatial characteristics. J. Arid. Environ. 71, 201–215.
Qiao, Juan, Zhang, Qiang, Zhang, Jie, et al., 2010. Comparison of atmospheric boundary layer in winter and summer over arid region of northwest China. J. Desert Res. 02, 422–430.
Renno, N.O., 2008. A thermodynamically general theory for convective vortices. Tellus 60A, 688–699.
Renno, N.O., et al., 2004. MATADOR 2002: a pilot field experiment on convective plumes and dust devils. J. Geophys. Res. 109 http://dx.doi.org/10.1029/2003JE002219. E07001.
Renno, N.O., Ingersoll, A.P., 1996. Natural convection as a heat engine: a theory for CAPE. J. Atmos. Sci. 53, 572–585.
Renno, N.O., Burkett, M.L., Larkin, M.P., 1998. A simple thermodynamical theory for dust devils. J. Atmos. Sci. 55, 3244–3252.
Roberts, A.J., Knippertz, P., 2014. The formation of a large summertime Saharan dust plume: convective and synoptic-scale analysis. J. Geophys. Res. Atmos. 119.4, 1766–1785.
Ryan, J.A., Carroll, I.J., 1970. Dust devils wind velocities: mature state. J. Geophys. Res. 75, 531–541.
Sinclair, P.C., 1969. General characteristics of dust devils. J. Appl. Sci. 30, 1599–1619.
Shapiro, A., Kogan, Y., 1994. On vortex formation in multicell convective clouds in a shear-free environment. J. Atmos. Res. 33, 125–136.
Shen, Jianguo, Zhaobo, Sun, Zhang, Qiuying, et al., 2008. Preliminary study on dust emission rate over arid steppe area. J. Desert Res. 28 (6), 1045–1049.
Shen, Zhibao, Shen, Yanbo, Du, Mingyuan, et al., 2003. Observational result of dust emission rate over sand surface of Gobi desert during dust storm. Plateau Meteorol. 22 (6), 545–550.
Shi, G.Y., Zhao, S.X., 2003. Several scientific issues of studies on the dust storms. Chin. J. Atmos. Sci. 27 (4), 591–606.
Song, L., Han, Y., Zhang, Q., et al., 2004. Monthly temporal-spatial distribution of sandstorms in China as well as the origin of Kosa in Japan and Korea. Chin. J. Atmos. Sci. 28 (6), 820–827.
Sun, J.M., Ding, Z.L., Liu, T.S., 1998. Desert distributions during the glacial maximum and climatic optimum: example of China. Episodes 21, 28–31.
Toigo, A.D., 2003. Numerical simulation of Martian dust devils. J. Geophys. Res. 108 (E6), 11–14.
Wang, Jiang, 2011. Characteristics of climate change for wind in recent 55 years in

Xinjiang. Public Commun. Sci. Technol. 21, 66–67.
Yang, Xinghua, He, Qing, Mamtimin, Ali, 2010. Estimation of sand transport flux during a sandstorm in Tazhong. Arid Zone Res. 6, 969–974.
Zhang, Qiang, Guoan, Wei, Hou, Ping, 2004. Observation studies of atmosphere boundary layer characteristic over Dunhuang Gobi in early summer. Plateau Meteorol. 5, 587–597.
Zhang, Q., Zhang, J., Qiao, J., et al., 2011. Relationship of atmospheric boundary layer depth with thermodynamic processes at the land surface in arid regions of China. Sci. China Earth Sci. 41 (09), 1365–1374.